

논문 2005-42TE-2-3

센서 결합을 이용한 이동 로봇 제어

(Mobile Robot Control with Sensor Combination)

홍 선 학*

(Hong Seon Hack)

요 약

본 논문에서는 이동 로봇 주행의 경로 탐색에 장애가 되는 환경 인식의 불확실성을 감소시키기 위한 센서 결합 방식을 제시하였다. 광학식엔코더, 초음파센서(SRF04) 및, 적외선센서(GP2YA02YK)에서 수집된 데이터를 운동제어기(TMS320LF2407A)에서 처리하여 장애물을 감지하고, 안정적인 경로탐색을 계산할 수 있는 이동로봇 제어방식을 실험을 통하여 구현하였다.

Abstract

This paper represents the sensor combination technique of mobile robot to reduce the ambiguity and uncertainty of environment that prevents the mobile robot from recognizing the path planning and navigation. The sensors such as optical encoder, ultra sonar sensor, and infra-red sensor gathered the dynamic information of mobile robot that are used to detect the obstacle. Therefore, the mobile robot controller with sensor combination is stably demonstrated by the experimental results.

Keywords : Mobile Robot, Sensor Combination, TMS320LF2407A, Sonar Sensor, Navigation

I. Introduction

The need for sensor combination based mobile robot control has been increasing because the single sensor system can only provide the partial information and the usage of sensor combination has no limitations since the number of sensors are invented to identify the feature of objects.^[1]

If a mobile robot is operated in uncertain environments, multiple sensors have to be used and they reduce the ambiguity and uncertainty in making decisions. Solving the problem of self localization and map-updating make mobile robot control possible in

uncertain environment conditions.

The extended study of mobile robot navigation control uses the integrated exploration. Therefore localization and map updating are indispensable for mobile robot researches although they are also enable to apply path planning, navigation and tracking control methods.

Many kinds of sensor have been used to get the data from environment, and the interrelation between mobile robot and uncertain environment is calculated on the basis of the sensor information. There are many active researches to apply different kind of sensors for the self localization and obstacle detection. In this paper, the sensors such as rotary encoder, sonar and infrared sensors have been used to detect the obstacles in the navigation environment and update with sensor combination method were

* 정회원, 서일대학 정보기술계열
(Department of Computer Application Electronic
Engineering, SEOIL COLLEGE)
접수일자: 2005년3월25일, 수정완료일: 2005년6월2일

provided for the mobile robot control.

II. Basic Theory

This chapter surveys the sensors used in mobile robot control. The sensor informations that are gathered by the sonar, infra-red and optical encoder attached to the main wheel motors are coordinated to produce the robot position data for mobile robot navigation. And also the mobile robot is mechanically analyzed and constructed as a navigational vehicle. The systems of the mobile robot controller with sensors are schematically explained and tested by the experimental results.

1. Modeling for Position Data

Main wheel velocities are calculated by the 1000 pulses per revolution from the optical rotary encoder attached to the rotor of the main wheels. And at the same time, the incremental displacement between the sampling times is calculated by dead reckoning for the purpose of gathering the precise displacement and velocity information. Robot displacement D along the path of travel is given by the following equation.^[2]

$$D = \frac{D_L + D_R}{2} \quad (1)$$

Where D is the displacement of platform.

D_L is the displacement of left wheel from geometrical center.

D_R is the displacement of right wheel from geometrical center.

Similarly, the platform velocity is given by the following equation:

$$V = \frac{V_L + V_R}{2} \quad (2)$$

where V is the velocity of platform.

V_L is the velocity of left wheel.

V_R is the velocity of right wheel.

and according to the Fig 1, arc C_L represents a portion

of the circumference of a circle of radius $d + b$:

$$C_L = 2\pi(d + b) \quad (3)$$

where C_L is the circumference of a circle traced by left wheel.

d is the distance between left and right wheels.

b is the inner turn radius.

Combining the above equations and the relationship:

$$\frac{D_L}{C_L} = \frac{\theta}{2\pi} \text{ yields } C_L = \frac{2\pi D_L}{\theta}. \quad (4)$$

Solving for θ :

$$\theta = \frac{D_L}{d + b} \quad (5)$$

Similarly, the shorter arc D_R represents a portion of the circumference of a circle of radius b :

$$C_R = 2\pi b \quad (6)$$

where C_R is the circumference of a circle traced by right wheel.

Combining the above equation and the relationship:

$$\frac{D_R}{C_R} = \frac{\theta}{2\pi} \text{ yields } C_R = \frac{2\pi D_R}{\theta} \quad (7)$$

Solving for b :

$$b = \frac{D_R}{\theta} \quad (8)$$

Substituting this expression for b into the previous equation for θ , and the relationship is derived in Eq(9).

$$\theta = \frac{D_L}{d + \frac{D_R}{\theta}} = \frac{D_L - D_R}{d} \quad (9)$$

Although the variable of d in the denominator represents a serious error source because of uncertainties with floor contacts of navigation, it is well known from this expression that the vehicle

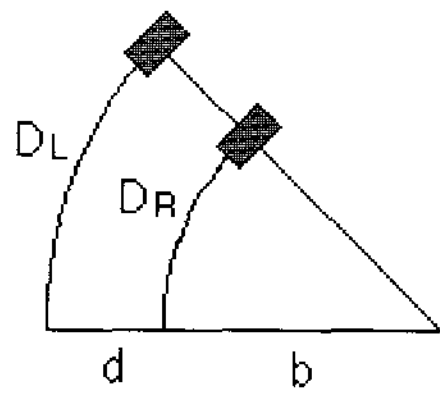


그림 1. 이동 로봇의 바퀴 궤적
Fig. 1. Wheel Traces of Mobile Robot.

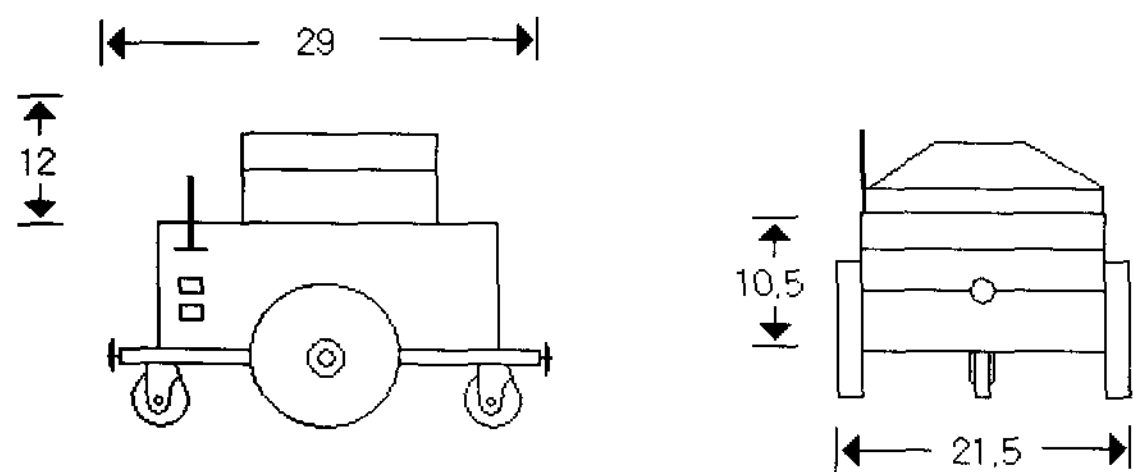


그림 2. 이동 로봇의 구조
Fig. 2. Details of Mobile Robot.

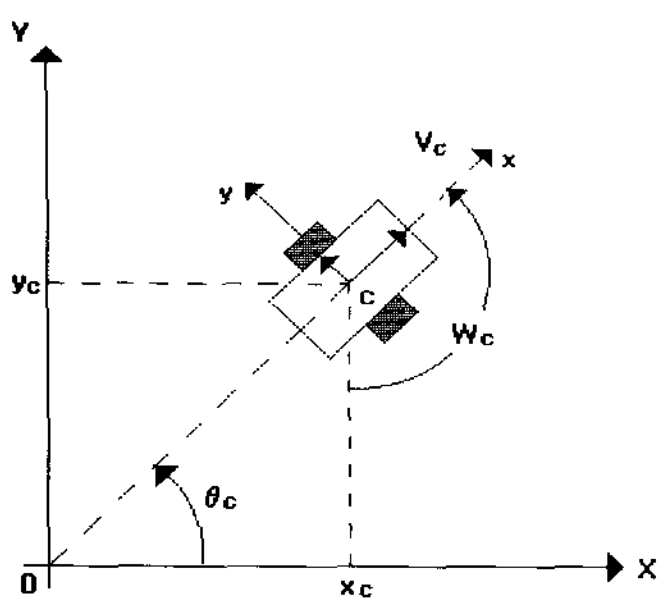


그림 3. 이동 로봇의 좌표
Fig. 3. Coordinate of Mobile Robot.

operation θ is a function of the displacements between left and right drive wheels and is completely independent of the driving path.

2. Configuration of Mobile Robot

The mobile robot based on this paper is shown in Fig 2.

3. Kinematics of Mobile Robot

Movement of mobile robot is described as Fig 3 in cartesian coordinates.^[3]

There are absolute coordinate X-Y and local coordinate x-y centered on geometrical center of mobile robot C. And therefore, it is possible to

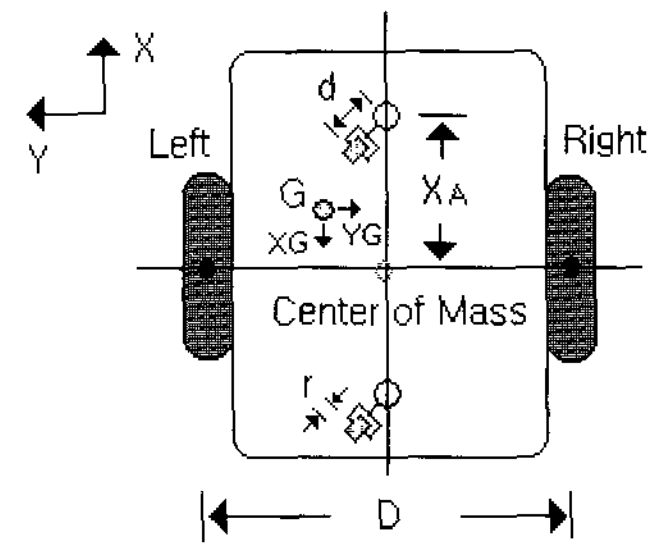


그림 4. 이동 로봇의 상부 모습
Fig. 4. Top down view of Mobile Robot.

표 1. 이동 로봇의 기계적인 차원
Table 1. Mechanical dimensions of mobile robot.

Descriptions	Symbol	Dim
Distance between the center of each wheels	D	0.235m
Distance between the rotational center and the contact point of caster with surfaces	d	0.001
Distance between center and caster in X axis	X_A	0.12
Radius of main wheel	r_w	0.07
Radius of caster wheel	r_A	0.012
Mass of mobile robot	M_m	22.3Kg
Mass of main wheel	M_w	1.2Kg
Mass of caster wheel	m_c	0.75Kg

introduce the P vector with 3 degree of freedom to denote the relationship between absolute and local coordinates.

$$P_c = \begin{bmatrix} X_c \\ Y_c \\ \theta_c \end{bmatrix} \quad (10)$$

where angle θ_c is rotated angle from X axis of global coordinates to x axis in local coordinates in counterclockwise direction. There are 2 postures, one of which is the fixed reference posture and the other is the current robot posture of geometrical center of robot. So the posture of robot, P, is described as

function of time $t(x(t), y(t))$, which is called path trajectory. Geometrical configuration of the mobile robot for this paper is shown Fig 4. There are two main wheels at both sides of the robot center driven by DC servo motor with optical encoders and 2 casters. Mobile robot is controlled by the different speeds of the two DC brush type motors attached at the center of mobile robot. Auxiliary casters are smaller than main wheels shown in the Fig 4. The mass center is not concentrated on the geometrical center C but on the mass center G except the mass of wheels including casters with the mass center in Z direction neglected.

The nomenclature of mobile robot is listed in Table 1.

The relationship between global coordinate(X-Y coordinate) and local coordinate(x-y coordinate) is derived in Eq(11).

$$\begin{aligned} X &= x \cos \theta_c - y \sin \theta_c + X_c \\ Y &= x \sin \theta_c + y \cos \theta_c + Y_c \end{aligned} \quad (11)$$

or, in matrix form as Eq(12).

$$\begin{bmatrix} x \\ y \end{bmatrix} = \begin{bmatrix} \cos \theta_c & \sin \theta_c \\ -\sin \theta_c & \cos \theta_c \end{bmatrix} \begin{bmatrix} X - X_c \\ Y - Y_c \end{bmatrix} \quad (12)$$

Denoting the pose and velocity of the robot as P_c and \dot{P}_c , we can derive following Eq(13) and Eq(14).

$$P_c = \begin{bmatrix} X_c \\ Y_c \\ \theta_c \end{bmatrix} \quad (13)$$

$$\begin{aligned} \dot{P}_c &= \begin{bmatrix} \dot{X}_c \\ \dot{Y}_c \\ \dot{\theta}_c \end{bmatrix} = \\ \begin{bmatrix} v_c \cos \theta_c \\ v_c \sin \theta_c \\ \omega_c \end{bmatrix} &= \begin{bmatrix} \cos \theta_c & 0 \\ \sin \theta_c & 0 \\ 0 & 1 \end{bmatrix} \begin{bmatrix} v_c \\ \omega_c \end{bmatrix} = J_a \quad (14) \end{aligned}$$

Where Jacobian matrix converts velocity and angular acceleration of robot into velocity and acceleration in absolute coordinates.

표 2. 주 제어 전동기 정격

Table 2. Specifications of Main control motor.

Items	Descriptions
Rate Voltage(V)	24
Rate Current(A)	2.1
Rate Speed(rpm)	3000
Torque Constant(kg-cm)	0.08
Amateur Resistance(Ω)	2.7
Rate Torque(kg-cm)	1.0
Gear ratio	1/10

4. The model of Mobile Robot

The specifications of main wheel motor in Table 2 are used for deriving the motor dynamic equations as following.^[4]

Motor parameters are calculated referring to the Table 2.

$$\tau_m = \frac{R_a J_M}{(R_a B + n K_t K_b)} = 2.4[\text{sec}]$$

$$K_M = K K_t = 2.4 \times 0.78 = 1.88$$

Moment of inertia for mobile robot is calculated.

$$\hat{A} = 12.95 (kgm^2), \hat{B} = 0.10473 (kgm^2)$$

So the plant model of the mobile robot is written as Eq (15).

$$\begin{aligned} W_c(s) &= \frac{1}{2(\hat{A}\hat{B})S} \frac{2\hat{B}K_M}{\tau_M S + 1} \frac{K_D S^2 + K_P S + 1}{S} W_E \\ &= \frac{0.145}{S(2.4S + 1)} \frac{K_D S^2 + K_P S + K_I}{S} W_E \quad (15) \end{aligned}$$

III. Map-Based Positioning

There are three basically different approaches for measuring the distance. First sensors based on measuring the time of flight(TOF) of a pulse of emitted energy traveling to a reflecting object, then echoing back to a receiver. Second the phase-shift measurement ranging technique involves continuous

wave transmission as opposed to the short pulsed outputs used in TOF systems. And finally, sensors based on frequency-modulated (FM) radar. In this paper, the time of flight(TOF) method is adopted for the purpose of collision avoidance. The measured pulses typically come from an ultrasonic energy source. Therefore, the relevant parameters involved in range calculation are the speed of sound in air(roughly 0.3m/ms). Using elementary physics, distance is determined by multiplying the velocity of the energy wave by the time required to travel the round-trip distance.^[5,6,7]

$$d = v \times t \tag{16}$$

where d = round trip distance

v = speed of propagation

t = elapsed time

The measured time is representative of traveling twice the separation distance (i.e., out and back) and must therefore be reduced by half to result in actual range to the target. The advantage of TOF systems arise from the direct nature of their straight-line active sensing. The returned signal follows essentially the same path back to a receiver located coaxially with or in close proximity to the transmitter. The absolute range to an observed point is directly available as output with no complicated analysis required, and the technique is not based on any assumptions concerning the particular properties or orientation of the target surface. In this paper, the SRF04 ultra-sonic rangefinders are used. The SRF04 only need to supply a short 10uS pulse to trigger input to start the ranging. The SRF04 would send out an 8 cycle burst of ultrasound at 40khz and raise its echo line high. It then listens for an echo, and as soon as it detects one it lowers the echo line again. The echo line is therefore a pulse whose width is proportional to the distance to the object. By timing the pulse it is possible to calculate the range in centimeters or anything else. If nothing is detected then the SRF04 will lower its echo line anyway about 36mS. In fact,

it is possible in some cases for the transmitting and receiving transducers to be the same device. The absolute range to an observed point is directly available as output with no complicated analysis required, and the technique is not based on any assumptions concerning the planar properties or orientation of the target surface.

The missing part problem seen in triangulation does not arise because minimal or no offset distance between transducers is needed. Furthermore, TOF sensors maintain range accuracy in a linear fashion as long as reliable echo detection is sustained, while triangulation schemes suffer diminishing accuracy as distance to the target increases.

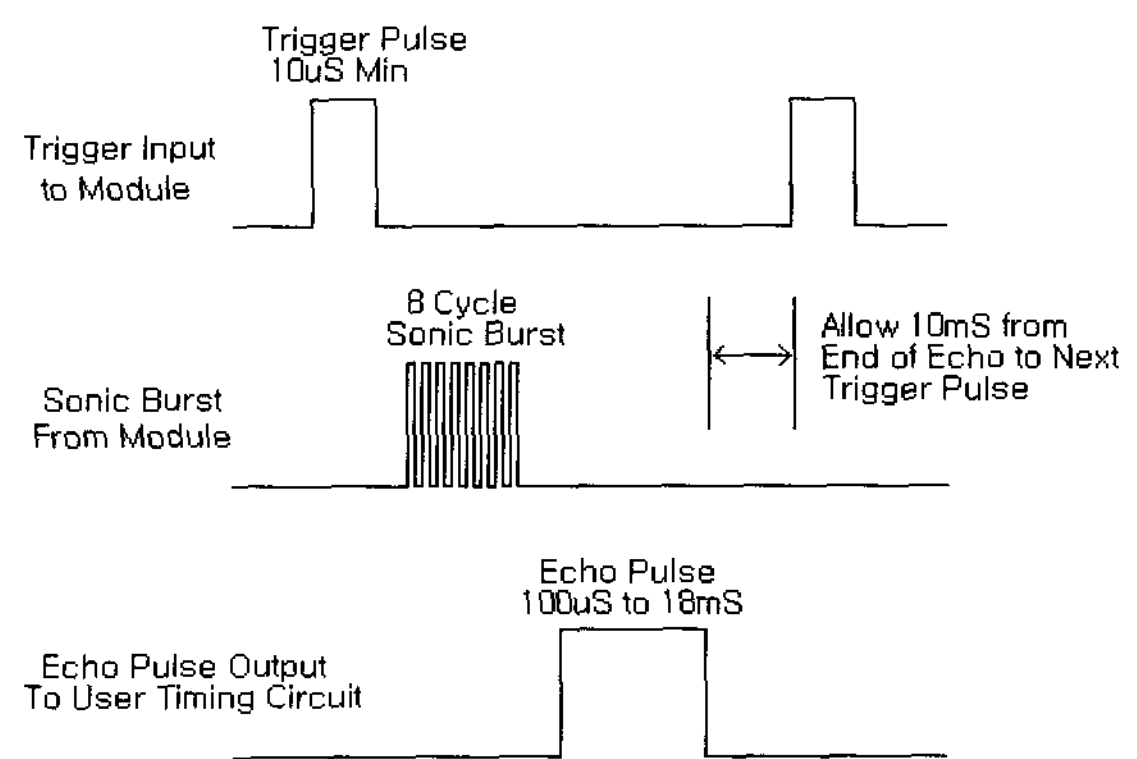


그림 5. SRF04 타이밍도
Fig. 5. SRF04 Timing Diagram.

1. Hardware configuration of control system

The control system for mobile robot is shown in Fig 6 as following.^[8,9]

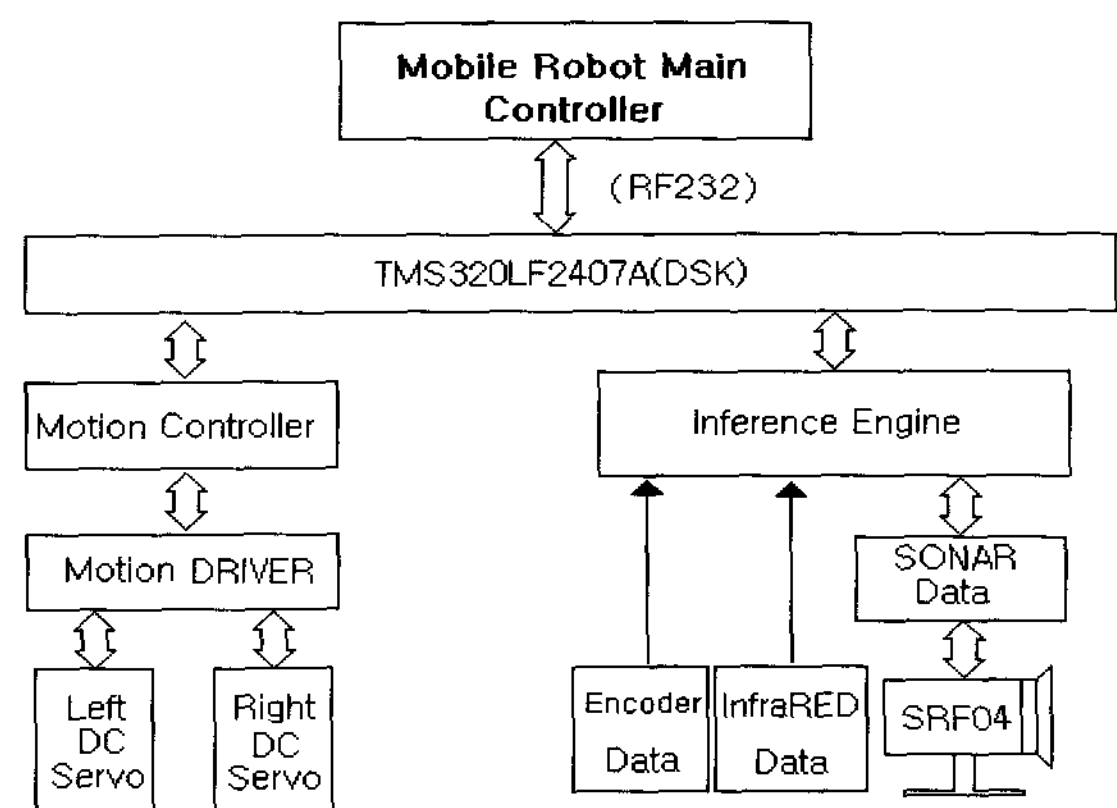


그림 6. 제어 시스템의 블록도
Fig. 6. Block of Control System.

The main controller consists of IBM-PC(Pentium 4, Win-XP), and motion controller is installed to control main wheel DC motors and to process the data from sensor combination units which are sonar sensor, infrared sensor and optical encoder. Independently operating, the sonar and infrared sensors are devised to generate the local information around mobile robot in real time through wireless RF232C port.^[10,11]

2. Characteristics of Motion controller

The debugging and emulating tests are executed on the controller based on IBM PC in stand alone mode. Motion controller, which is possible to do coordinate motion based on the TMS320LF2407A (30MIPS, C2000 Code Composer), controls the robot motion to execute maneuvering such as obstacle avoidance, and autonomous navigation by sensor combination in door environments. Motion control schemes basically control mobile robot by differential steering based on the position and velocity data by the optical encoders and wireless communication through RF232C port.^[12,13,14]

IV. Experiments of Sensor combination

The ultrasonic ranging system is developed by making usage of the time of flight of sonar on purpose with SRF04 units. Also it extracts the features such as distance and target types based on the obtained raw data and finally recognize an environment. The infrared sensor(GP2Y0A02YK) is adopted to discern the characteristics of short distance things. It distinguishes the features of target type between 20cm and 150cm. And it is less influence on the colors of reflected objects and their reflectivity, due to optical triangle measuring method. Sequentially operating, these units are communicated to main controller through RF232C channels and the latest obtained information of an environments is sent to the main controller. The main controller obviously operates the robot by the sensor combination, the obstacle avoidance and the path planning.

Fig 7(a) and Fig 7(b) show the acquired data with sensor combinations such as sonar and infra-red sensor, where the sampling data according to the distance changes.^[15,16]

V. Conclusions

The dynamics of mobile robot are derived from which the open loop transfer function between velocity and real output are written as Eq(17).

$$W_C = \frac{0.145}{S(2.4S + 1)} \frac{K_D S^2 + K_P S + K_I}{S} W_E \quad (17)$$

The step responses of above equation simulated by MATLAB is shown in Fig 8(a) and the Nyquist plot in Fig 8(b).

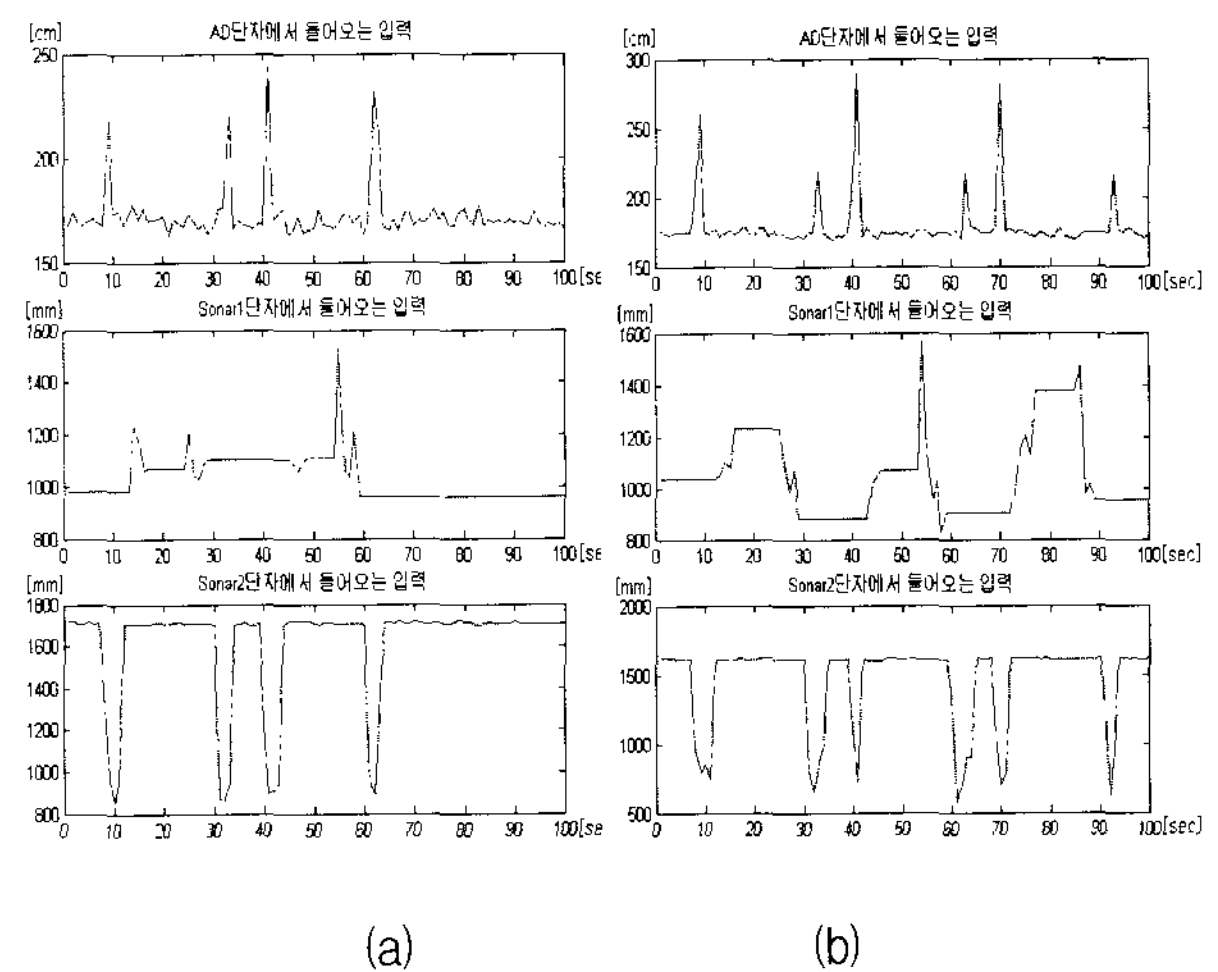
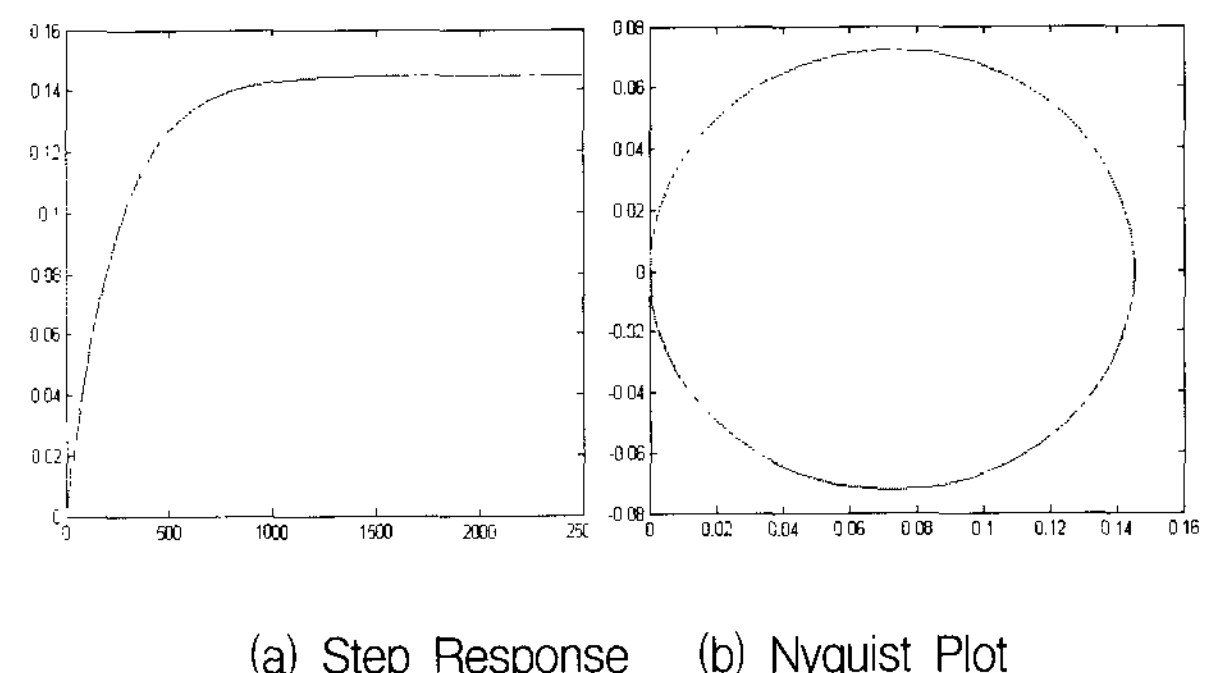


그림 7. 센서 결합 파형

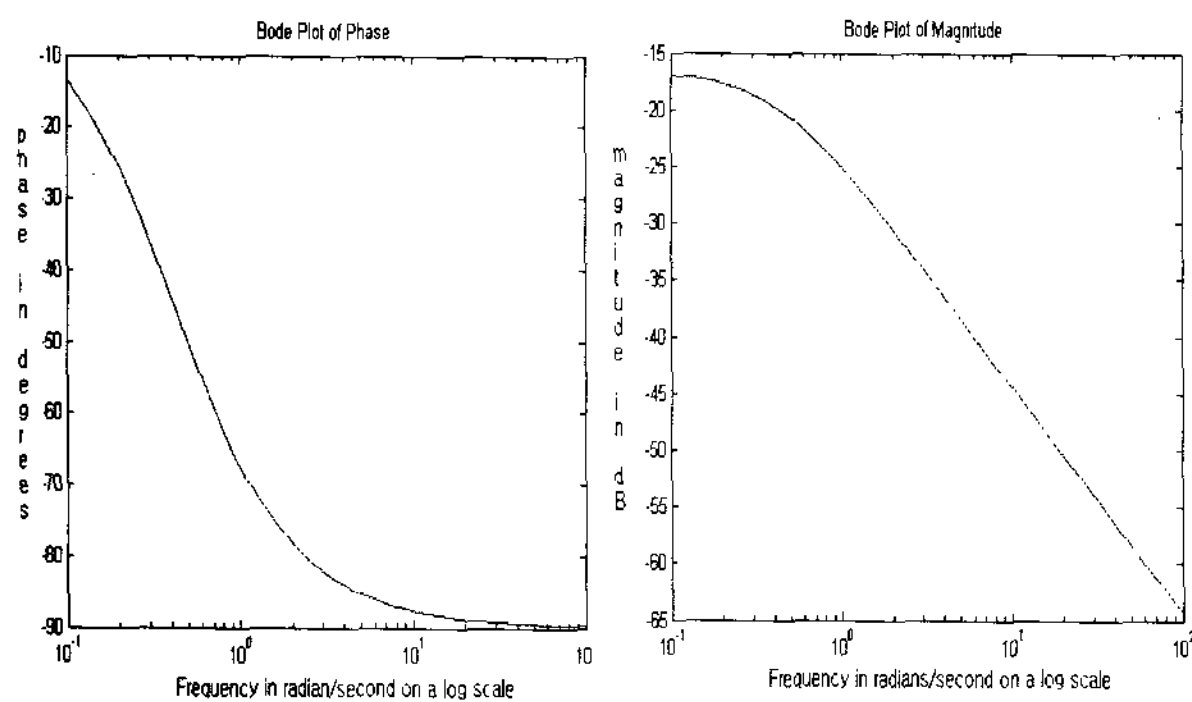
Fig. 7. Sensor Combination waveforms.



(a) Step Response (b) Nyquist Plot

그림 8. 되먹임을 갖는 특성 곡선

Fig. 8. Characteristics curve with feedback.



(a) Bode plot phase

(b) Bode plot magnitude

그림 9. 주파수 응답 곡선

Fig. 9. Frequency response plots.

$$(K_P = 1, K_D = 0, K_I = 0)$$

There are a number of equivalent possibilities, the most common being to plot $20 \log_{10} |H(j\omega)|$ versus ω and $\angle H(j\omega)$ versus ω on linear scales and ω on a log scale. The quantity $20 \log_{10} |H(j\omega)|$ is called the decibel, or dB, gain of the frequency response $H(j\omega)$. See Fig 9. for the Bode plots for open loop transfer function of mobile robot.^[17,18]

References

- [1] Gordon McComb, Robot Builder's Bonanza, TAB Books, 1987.
- [2] JOHN J. CRAIG, Introduction to ROBOTICS, Addison-Wesley Pub co. 1989.
- [3] Saeed B. Niku, Introduction to Robotics, Prentice Hall, 2001.
- [4] T. Kenjo, Power Electronics for the Micro processor age, Oxford Pub, 1990.
- [5] Petruzella, Industrial Electronics, McGraw-Hill, 1996.
- [6] J. Michael Jacob, Industrial Control Electronics, Prentice-Hall, 1989.
- [7] James Maas, Industrial Electronics, Prentice-Hall, 1995.
- [8] Frank L. Lewis, Optimal Estimation, John Wiley & Sons, 1986.
- [9] Hans Butler, Model Reference Adaptive Control, Prentice-Hall, 1992.
- [10] Bernard, Adaptive Signal Processing, Prentice-Hall, 1985.
- [11] R. Isermann, Adaptive Control Systems, Prentice-Hall, 1992.
- [12] S. B. Dewan, Power Semiconductor Circuits, 1987.
- [13] Peter vas, Vector Control of Electric machine, Clarendon Press, 1990.
- [14] An Introduction to ROBOT TECHNOLOGY, Philippe Coiffet, 1982.
- [15] TMS320LF2407 DSK Technical Reference, Digital Spectrum, 2000.
- [16] 홍선학, 제어계측공학, 성안당, 2001.
- [17] J. S. R. Jang, Neuro-Fuzzy and Soft Computing, 1997.
- [18] Contemporary Linear Systems, Using MATLAB, Robert S. Strum, 1994.

저 자 소 개



홍 선 학 (정회원)

1985년 광운대학교 전기공학과 학사졸업.

1988년 광운대학교 전기공학과 석사졸업.

1994년 광운대학교 대학원 박사 졸업.

<주관심분야 : 제어, 컴퓨터응용, 로봇분야>